Error Propagation Analysis in Color Measurement and Imaging

Peter D. Burns,[1,2]* Roy S. Berns[1]

[1] Munsell Color Science Laboratory, Center for Imaging Science, Rochester Institute of Technology, 54 Lomb Memorial Drive, Rochester, New York 14623-5604

[2] Eastman Kodak Company, Imaging Research and Development Laboratories, Rochester, New York 14650-1925

Received 11 September 1996; accepted 11 January 1997

Abstract: We apply multivariate error-propagation analysis to color-signal transformations. Results are given that indicate how linear, matrix, and nonlinear transformations influence the mean, variance, and covariance of color-measurements and color-images. Since many signal processing paths include these steps, the analysis is applicable to color-measurement and imaging systems. Expressions are given that allow image noise or error propagation for a spectrophotometer, colorimeter, or digital camera. In a computed example, error statistics are propagated from tristimulus values to CIELAB coordinates. The resulting signal covariance is interpreted in terms of CIELAB error ellipsoids and the mean value of color-difference measures, ΔE^*_{ab} and ΔE^*_{94}. The application of this analysis to system design is also illustrated by relating a ΔE^*_{94} tolerance to equivalent tristimulus-value error statistics. © *1997 John Wiley & Sons, Inc. Col Res Appl, 22, 280–289, 1997*

Key words: CIELAB; CIE94; color error; color camera; color calibration; image noise

INTRODUCTION

During the specification, design, and use of color-measurement and color-image acquisition systems, much attention is given to the ability to capture and preserve the required color information. Once acquired, it is common to transform detected signal data between color spaces, e.g., between spectral radiance, tristimulus values, or camera signals and CIELAB or CIELUV coordinates. Similar transformations are performed during the calibration of both color-measurement and imaging systems.

Uncertainty or noise in a detected or recorded color signal can arise from many sources, e.g., detector dark current, exposure shot noise, calibration variation, or varying operating conditions. If a physical model of the system and its associated signal processing is available, the influence of various sources on system performance can be understood for both color-measurement[1–8] and imaging applications.[9–12] In addition, statistical aspects of human vision can also be explicitly included in the analysis.[13] This approach allows the comparison of design/technology choices in terms of system performance requirements, e.g., color error or signal-to-noise ratio. We consider the case of general stochastic error sources, which can be functions of exposure level, wavelength, etc.

Measurements of systematic error are often used to evaluate accuracy during system calibration. Methods of correcting for systematic measurement error due to spectral bandpass, wavelength scale, and linearity[14–16] have been reported. From a statistical point of view this type of error represents bias, since the mean signal is not equal to the true value.

To address system precision we need to understand the origin and propagation of signal uncertainty.[17–20] This would, for example, allow the comparison of observed performance in a secondary color-space with that limited by measurement error, or image detection, in an original signal-space. The magnitude of errors introduced by approximations to functional color-space transformations[21,22] could also be compared with intrinsic errors.

Several workers[1–6] have addressed error propagation from instrument reading to chromaticity coordinates. In addition, propagation of uncorrelated measurement errors in the nonlinear colorimetric transformations from tristimulus values to perceptual color spaces has also been described.[7,8]

In this article we extend the above analysis to include the effect of correlation between the uncertainty in related

* Correspondence to: Peter D. Burns, Eastman Kodak Company, Mail Stop 01925, Rochester, NY 14650-1925 or pburns@Kodak.com

sets of color signals. As Nimeroff has shown,[3] the correlation is needed when computing error ellipses for 2-dimensional color-space projections, such as chromaticity coordinates. In addition, this information can be important if colorimetric measurements are used to derive statistical color models of processes or mechanisms. If stochastic errors are propagated through various color-signal transformations, then their magnitude can be compared with that attributable to the process or sample under study.

Our analysis is given in a functional and matrix-vector notation, to aid in its broad application to color measurement, calibration, and color-image processing. While this approach is now common in color modeling,[23–26] it is rarely used in color-error propagation.[19] Many previously published reports on the subject can be seen as special cases of the general approach taken in this article. The results are applied to several specific common transformations from spectrophotometric colorimetry and CIELAB color specification. In addition we show how stochastic color errors influence the mean value of color-difference measures, ΔE^*_{ab} and ΔE^*_{94}.

ERROR PROPAGATION

Univariate Transformation

If a signal is subject to an error we can think of a measurement as a random variable. For example, if a signal value x is detected for a process or image whose true value is K, we can represent the set of measurements as

$$x = \mu_x + e_x,$$

where e_x is a zero-mean random variable with a probability density function, corresponding variance, σ_x^2, and mean value, μ_x. If x is an unbiased measurement of the physical process, then the mean value is equal to K. If we transform the original signal,

$$y = f(x),$$

then y will also be a random variable. If $f(x)$ and its derivatives are continuous, the statistical moments of y can be approximated in terms of the original moments, μ_x, σ_x^2, and $f(x)$. This is done by expanding the function in a Taylor series about the mean value, μ_x, and expressing the first and second moments of y in terms of those of x. The mean value of y is given by[17,18]

$$\mu_y = E[f(x)] \cong f(\mu_x) + \tfrac{1}{2}[f''_{xx}\sigma_x^2], \qquad (1)$$

where $E[\cdot]$ is the statistical expectation and

$$f''_{xx} = \left.\frac{\partial f^2(x)}{\partial^2 x}\right|_{\mu_x}.$$

Equation (1) indicates that the expected value of $f(x)$ is equal to the function evaluated at its mean value, but with the addition of a bias that is the product of the second derivative of f and the variance of x. For many applications the second, bias term is small compared to the first. We will adopt this assumption except as noted.

An expression for the variance of y can be similarly found. Following this approach[17–20] it can be shown that

$$\sigma_y^2 \cong f_x'^2\sigma_x^2 + \frac{f''^2_{xx}}{4}(E[(x-\mu_x)^4] - \sigma_x^4), \qquad (2)$$

where f'_x is the first derivative of f with respect to x evaluated at μ_x. If x is, or can be appoximated by, a normal random variable, then $E[(x-\mu_x)^4] = 3\sigma_x^4$ and Eq. (2) becomes

$$\sigma_y^2 \cong f_x'^2\sigma_x^2 + \frac{f''^2_{xx}}{2}\sigma_x^4. \qquad (3)$$

The usual expression for σ_y^2 includes only the first term of the RHS of the previous Eqs. (2) and (3),

$$\sigma_y^2 \cong f_x'^2\sigma_x^2. \qquad (4)$$

In most cases relevant to color-measurement and color-image processing, this term is the dominant one, but there may be mean values for which this is not a good approximation. We will assume Eq. (4) unless stated otherwise. This shows that for a univariate transformation, the signal variance is scaled by the square of the first derivative of the function, evaluated at the mean value.

Multivariate Linear Transformation

A common color-signal transformation is a matrix operation, e.g.,

$$\mathbf{y} = \mathbf{A}\mathbf{x},$$

where a set of input signals $\{x_1, x_2, \ldots, x_n\}$ is written as $\mathbf{x}^T = [x_1 x_2 \cdots x_n]$ and the output is $\mathbf{y}^T = [y_1 y_2 \cdots y_m]$. The superscript, ^{T}, indicates matrix transpose, and $\mathbf{A}$ is the (mxn) matrix of weights. If each member of the set $\{x\}$ is a random variable, the second-order moments can be written as a covariance matrix;

$$\Sigma_x = \begin{bmatrix} \sigma_{11} & \sigma_{12} & \cdots & \sigma_{1n} \\ \sigma_{21} & \sigma_{22} & \cdots & \\ \vdots & & \ddots & \\ \sigma_{n1} & & & \sigma_{nn} \end{bmatrix},$$

where $\sigma_{11} \equiv \sigma_{x_1}^2$, and the covariance between x_1 and x_2 is σ_{12}. If the set of signals $\{x\}$ are statistically independent, Σ_x is diagonal. The resulting covariance matrix for $\mathbf{y}$, from multivariate statistics,[19,27] is given by

$$\Sigma_\mathbf{y} = \mathbf{A}\Sigma_\mathbf{x}\mathbf{A}^T. \qquad (5)$$

Equation (5) can also be written as an equivalent set of linear equations. For example, Wyszecki and Stiles[28] address such matrix transformations and their effect on color-matching ellipsoids.

Multivariate Nonlinear Transformation

When multivariate signals are transformed and combined, we can express the resulting transformation of the covariance matrix as a combination of the above two cases. We start with a set of input signals with covariance matrix, Σ_x. Each of the signals is transformed,

$$\begin{aligned} y_1 &= f_1(x_1, x_2, \ldots, x_n) \\ y_2 &= f_2(x_1, x_2, \ldots, x_n), \\ &\vdots \end{aligned} \tag{6}$$

where f may represent a compensation for detector response, or a nonlinear transformation between color spaces. Let the matrix derivative operator be

$$\mathbf{J_f(x)} = \begin{bmatrix} \frac{\partial y_1}{\partial x_1} & \frac{\partial y_1}{\partial x_2} & \cdots & \frac{\partial y_1}{\partial x_n} \\ \frac{\partial y_2}{\partial x_1} & \ddots & & \\ \vdots & & \ddots & \\ \frac{\partial y_n}{\partial x_1} & & & \frac{\partial y_n}{\partial x_n} \end{bmatrix},$$

where each element of $\mathbf{J}_{f(\mathbf{x})}$ is evaluated at the mean, $(\mu_{x_1}, \mu_{x_2}, \ldots, \mu_{x_n})$. This notation is that of Sluban and Nobbs,[29] and this operator is the Jacobian matrix.[30] The transformation of the covariance matrix due to Eq. (6) is given by[19]

$$\Sigma_{\mathbf{y}} \cong \mathbf{J}_{f(\mathbf{x})} \Sigma_{\mathbf{x}} \mathbf{J}^T_{f(\mathbf{x})}. \tag{7}$$

Equation (7) can also be written[20]

$$\sigma_{y_{ii}} \cong \sum_{j=1}^{n} \left(\frac{\partial f_i}{\partial x_j} \right)^2 \sigma_{x_{jj}} + 2 \sum_{j=1}^{n-1} \sum_{k=j+1}^{n} \frac{\partial f_i}{\partial x_j} \frac{\partial f_i}{\partial x_k} \sigma_{x_{jk}},$$

which is the form most often used. Note that the simpler univariate and matrix results of Eqs. (4) and (5) are special cases of Eq. (7).

Many color-signal transformations can be seen as a cascading of the above types of transformations. We now demonstrate this by developing specific expressions for error propagation from spectral reflectance data to tristimulus values. This is followed by the transformation to CIELAB coordinates. These are important and common transformations, but can also be prototypes for image processing steps found in many electronic imaging systems.

SPECTROPHOTOMETRIC COLORIMETRY

A fundamental color transformation is that between instrument spectral measurement data and the corresponding colorimetric coordinates. If one is using a spectrophotometer, this involves measuring the spectral reflectance factor at several wavelengths over the visible range. These are weighted with an illuminant spectral power distribution, and combined in the form of the three tristimulus values. Often these data are then transformed into a perceptual color space such as CIELAB or CIELUV. The following analysis addresses noise propagation through this signal-processing path.

Error in Tristimulus Values

The tristimulus values are calculated by multiplying the measured sample spectral reflectance factor by a CIE illuminant and color-matching function weighting at each wavelength. A summation of the result yields the three tristimulus values. For the first tristimulus value this is expressed as

$$X = k\Delta\lambda \sum_{j=1}^{jmax} s_j \bar{x}_j R_j,$$

where $\bar{x}_j$ is the first CIE color-matching function, s is the illuminant spectral power distribution, $\Delta\lambda$ is the wavelength sampling interval, R is the sampled spectral reflectance factor, and k is a normalizing constant.

The calculation of the tristimulus values can be expressed in matrix notation,

$$\mathbf{t} = k\Delta\lambda \mathbf{M}^T \mathbf{S} \mathbf{r}, \tag{8}$$

where

$$\mathbf{t} = \begin{bmatrix} X \\ Y \\ Z \end{bmatrix}, \quad \mathbf{S} = \begin{bmatrix} s_1 & & & 0 \\ & s_2 & & \\ & & \ddots & \\ 0 & & & s_n \end{bmatrix}, \mathbf{r} = \begin{bmatrix} R_1 \\ R_2 \\ \vdots \\ R_n \end{bmatrix},$$

and $\mathbf{M}$ comprises the CIE color-matching functions,

$$\mathbf{M} = \begin{bmatrix} \bar{x}_1 & \bar{y}_1 & \bar{z}_1 \\ \vdots & \vdots & \vdots \\ \bar{x}_n & \bar{y}_n & \bar{z}_n \end{bmatrix}.$$

Often Eq. (8) is implemented using ASTM weights[31] that combine the illuminant and color matching function information,

$$\mathbf{t} = \mathbf{M}^T \mathbf{r}, \tag{9}$$

where $\mathbf{M}$ now indicates the weight matrix for a specified CIE illuminant.

The fact that the three color-matching functions overlap at various wavelengths introduces correlation into the error associated with the tristimulus elements of $\mathbf{t}$ (Ref. 1). If $\mathbf{t}$ is calculated as in Eq. (9), then the resulting covariance matrix is given as in Eq. (5):

$$\Sigma_{\mathbf{t}} = \mathbf{M}^T \Sigma_{\mathbf{r}} \mathbf{M}, \tag{10}$$

where $\Sigma_{\mathbf{r}}$ is the $(n \times n)$ spectral-reflectance covariance matrix. If the CIE color-matching functions and ASTM weights did not overlap, this result would revert to the uncorrelated error case. Note that, since the covariance

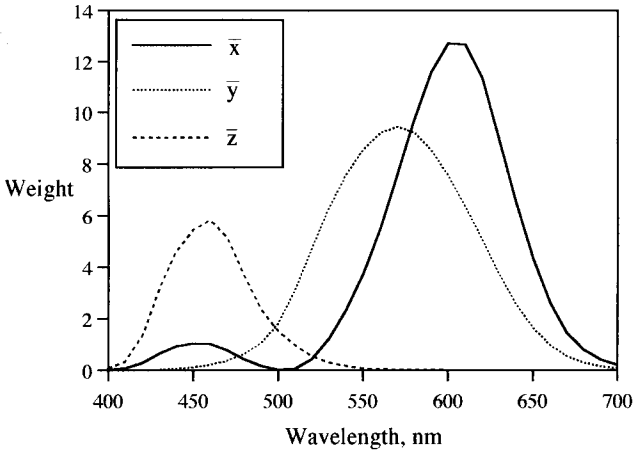

FIG. 1. ASTM, 10-nm weights for CIE Illuminant A, 2° observer.

matrix comprises the moments about the mean values of X, Y, Z, a constant bias error in $\{r\}$ has no effect on Σ_t.

Uncorrelated, Equal-Variance Instrument Errors

If we assume uncorrelated instrument errors, we can assess the effect of the overlapping color-matching functions alone on colorimetric error correlation. In this case the instrument error covariance matrix, Σ_r, is diagonal. To identify correlation introduced by the overlapping color-matching functions more easily, we consider the special case of uncorrelated and equal instrument error whose covariance matrix is

$$\Sigma_r = \sigma_r^2 \mathbf{I}, \tag{11}$$

where $\mathbf{I}$ is the diagonal identity matrix. This case could be used to model simple dark current error, or that due to quantization rounding. The resulting tristimulus-vector covariance matrix, Σ_t, is found by substituting Eq. (11) into Eq. (10),

$$\Sigma_t = \sigma_r^2 \mathbf{M}^T \mathbf{M}. \tag{12}$$

As an example, consider the case of the CIE illuminant A for the 2° observer, whose weights are plotted in Fig. 1. The tristimulus matrix that would result from uncorrelated instrument spectral reflectance error is calculated[32] from Eq. (12),

$$\Sigma_t = \sigma_r^2 \begin{bmatrix} 0.095 & 0.067 & 0.003 \\ 0.067 & 0.069 & 0.002 \\ 0.003 & 0.002 & 0.015 \end{bmatrix},$$

where the diagonal elements represent the variance of the error associated with the tristimulus values, X, Y, and Z. The corresponding correlation matrix is

$$\mathbf{R}_t = \begin{bmatrix} 1 & 0.826 & 0.071 \\ 0.826 & 1 & 0.069 \\ 0.071 & 0.069 & 1 \end{bmatrix}.$$

Thus, there is a correlation coefficient, $r_{xy} = 0.826$ between X and Y values, due to the overlapping weights.

CIELAB Errors

CIELAB coordinates, L^*, a^*, and b^*, are calculated from the tristimulus values, and those of a white object color stimulus[33] whose tristimulus values are X_n, Y_n, Z_n. For example, L^* is given by

$$L^* = 116 f(Y) - 16, \tag{13a}$$

where

$$f(Y) = \left(\frac{Y}{Y_n}\right)^{1/3} \quad \text{for } Y/Y_n > 0.008856$$

$$f(Y) = 7.787 \frac{Y}{Y_n} + \frac{16}{116}, \quad \text{for } Y/Y_n \le 0.008856. \tag{13b}$$

This indicates that L^* can be computed by first evaluating the nonlinear function Eq. (13b) and then the linear operation Eq. (13a).

The variance of the error in $f(Y)$ can be approximated as

$$\begin{aligned} \sigma^2_{f(Y)} &\cong \left(\frac{df(Y)}{dY}\right)^2 \sigma_Y^2 \\ &\cong \left(\frac{1}{3\mu_Y^{2/3} Y_n^{1/3}}\right)^2 \sigma_Y^2 \quad \text{for } \mu_Y/Y_n > 0.008856 \\ &\cong \left(\frac{7.787}{Y_n}\right)^2 \sigma_Y^2 \quad \text{for } \mu_Y/Y_n \le 0.008856. \end{aligned} \tag{14}$$

Here we assume that Y_n is a constant, but if we are interested in errors between laboratories or over time, then the measurement of the white object color stimulus can be a significant source of stochastic error.[8] In addition, the measured value of Y_n can introduce a bias error into all CIELAB values that are based on the measurement.

Equation (14) represents one element of the matrix operation of Eq. (7):

$$\Sigma_{f(t)} \cong \mathbf{J}_{f(t)} \Sigma_t \mathbf{J}^T_{f(t)},$$

where, for μ_X, μ_Y, $\mu_Z > 0.008856 Y_n$,

$$\mathbf{J}_{f(t)} = \frac{1}{3} \begin{bmatrix} \mu_X^{-2/3} X_n^{-1/3} & 0 & 0 \\ 0 & \mu_Y^{-2/3} Y_n^{-1/3} & 0 \\ 0 & 0 & \mu_Z^{-2/3} Z_n^{-1/3} \end{bmatrix}.$$

As stated previously, the error-propagation techniques used here apply strictly only to continuous functions with continuous derivatives. Clearly $f(Y)$ and its derivative functions are not continuous near $Y = 0.008856$, but evaluation of the function indicates that both $f(Y)$ and $df(Y)/dY$ are approximately continuous, to the limit imposed by the four digits of the constant 903.3. The second derivative function is discontinuous and error propagation analysis that includes this function could include verification of the error statistics in this region by direct simulation.

The corresponding calculations of a^* and b^* have a similar nonlinear first step and subsequent second step. The transformation to CIELAB can be expressed in matrix notation,

$$\begin{bmatrix} L^* \\ a^* \\ b^* \end{bmatrix} = \begin{bmatrix} 0 & 116 & 0 \\ 500 & -500 & 0 \\ 0 & 200 & -200 \end{bmatrix} \times \begin{bmatrix} f(X) \\ f(Y) \\ f(Z) \end{bmatrix} + \begin{bmatrix} -16 \\ 0 \\ 0 \end{bmatrix} \quad (15)$$

or

$$\mathbf{c} = \mathbf{N}\mathbf{f}(\mathbf{t}) + \mathbf{n},$$

where $\mathbf{c}$ is the CIELAB vector, $\mathbf{f}(\mathbf{t})$ represents the three univariate transformations, and $\mathbf{N}$ and $\mathbf{n}$ are the corresponding matrix and vector from Eq. (15). The covariance matrix for the error in the CIELAB values will be given by

$$\Sigma_{L^*a^*b^*} \cong \mathbf{N}\Sigma_{\mathbf{f}(\mathbf{t})}\mathbf{N}^T = \mathbf{N}\mathbf{J}_{\mathbf{f}(\mathbf{t})}\Sigma_{\mathbf{t}}\mathbf{J}^T_{\mathbf{f}(\mathbf{t})}\mathbf{N}^T. \quad (16)$$

CIELAB Chroma and Hue

In addition to distances in L^*, a^*, b^* space, visual color differences can also be expressed in the rotated rectangular differences in lightness, chroma, and hue, ΔL^*, ΔC^*_{ab}, ΔH^*_{ab} (Ref. 32). To express the covariance description of errors in L^*, a^*, b^* in terms of their transformed statistics, $\Sigma_{\Delta L^*\Delta C^*\Delta H^*}$, we first consider the transformation to lightness, chroma, and hue angle, h_{ab}. The chroma is

$$C^*_{ab} = \sqrt{a^{*2} + b^{*2}}$$

and the hue angle,

$$h_{ab} = \tan^{-1}\left(\frac{b^*}{a^*}\right).$$

We can again apply Eq. (7),

$$\mathbf{J}_{L^*C^*_{ab}h_{ab}} = \begin{bmatrix} 1 & 0 & 0 \\ 0 & \dfrac{\mu_{a^*}}{\mu_{C^*_{ab}}} & \dfrac{\mu_{b^*}}{\mu_{C^*_{ab}}} \\ 0 & -\dfrac{\mu_{b^*}}{\mu^2_{C^*_{ab}}} & \dfrac{\mu_{a^*}}{\mu^2_{C^*_{ab}}} \end{bmatrix},$$

where $\mu_{C^*_{ab}} = \sqrt{\mu^2_{a^*} + \mu^2_{b^*}}$, and

$$\Sigma_{L^*C^*_{ab}H_{ab}} \cong \mathbf{J}_{L^*C^*_{ab}h_{ab}}\Sigma_{L^*a^*b^*}\mathbf{J}^T_{L^*C^*_{ab}h_{ab}}. \quad (17)$$

The hue difference between two color samples is given by

$$\Delta H^*_{ab} = 2\sqrt{C^*_{ab_1}C^*_{ab_2}}\sin\left(\frac{\Delta h_{ab}}{2}\right), \quad (18)$$

where $C^*_{ab_1}$ and $C^*_{ab_2}$ are the two chroma values and Δh_{ab} is the hue-angle difference. To find the covariance matrix for the color-difference values, ΔL^*, ΔC^*_{ab}, ΔH^*_{ab}, involves only the additional transformation from Δh_{ab} to ΔH^*_{ab}. We are interested in hue differences about the mean, so the reference $C^*_{ab_1} = \mu_{C^*_{ab}}$ and $C^*_{ab_2}$ of Eq. (18) is taken as the ensemble of chroma values. Assuming small angles, Δh_{ab}, then

$$\Delta H^*_{ab} \approx \Delta h_{ab}\sqrt{\mu_{C^*_{ab}}C^*_2},$$

so

$$\mathbf{J}_{L^*,C^*_{ab},H^*_{ab}} = \begin{bmatrix} 1 & 0 & 0 \\ 0 & 1 & 0 \\ 0 & 0 & \mu_{C^*_{ab}} \end{bmatrix},$$

$$\Sigma_{\Delta L^*\Delta C^*_{ab}\Delta H^*_{ab}} \cong \mathbf{J}_{\Delta L^*\Delta C^*_{ab}\Delta H^*_{ab}}\Sigma_{L^*\Delta C^*_{ab}h_{ab}}\mathbf{J}^T_{\Delta L^*\Delta C^*_{ab}\Delta H^*_{ab}}. \quad (19)$$

The use of the above analysis will now be shown in a computed example of colorimetric error propagation.

COMPUTED EXAMPLE FOR COLORIMETER/CAMERA

Consider a tristimulus-filter colorimeter whose three spectral sensitivities are the CIE color-matching functions. The instrument, therefore, measures the sample tristimulus values directly. Let us also assume that the signal includes a random error whose rms value is 0.5% of full scale, i.e., 0.005. This error is uncorrelated between the X, Y, and Z signals. The variance of each signal is given by $(0.005)^2$, where the signal range is [0–1], or $\Sigma_t = 2.5 \times 10^{-5}\mathbf{I}$.

If we calculate the CIELAB coordinates from the measured data, the corresponding errors will be a function of the (mean) signals as in Eq. (14). As an example, let the true color tristimulus values be $X/X_n = 0.55$, $Y/Y_n = 0.5$, and $Z/Z_n = 0.05$, corresponding to a strong orange yellow. These values are on a [0–1] scale.

If we assume that the measurement errors are described or approximated by normal probability distributions, then the three-dimensional, 95% probability error ellipsoid is shown in Fig. 2. This is derived from the eigenvectors and eigenvalues of the covariance matrix, as is commonly done in multivariate statistics.[33] The ellipsoid represents a three-dimensional analog of the univariate 95% confidence interval about the mean, for the population of measurements $\{X, Y, Z\}$ whose variation is described by the covariance matrix Σ_t. The spherical shape is due to the independent and equal-variance nature of the errors for the three signals.

In applying Eq. (14b) for each tristimulus value,

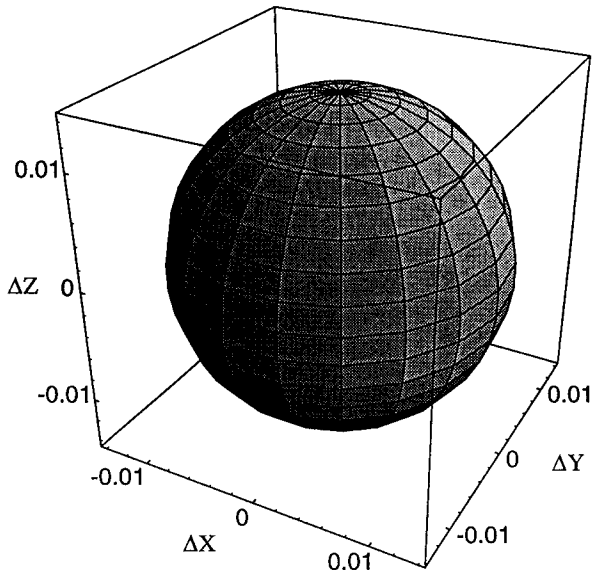

FIG. 2. Error ellipsoid (95%) for the measured tristimulus values example.

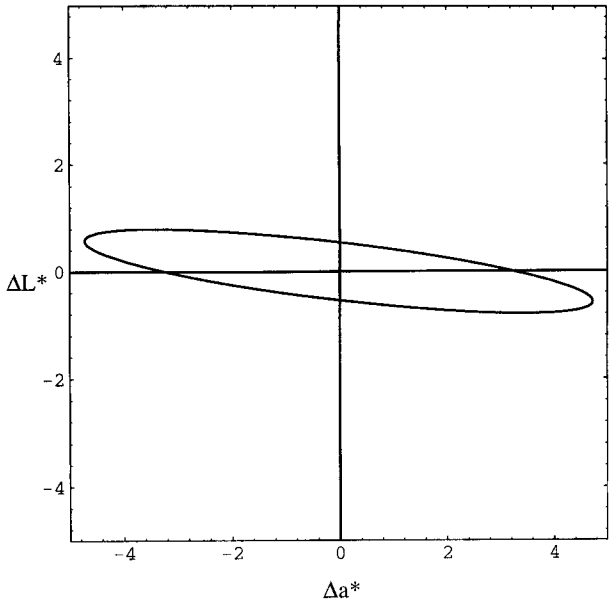

FIG. 3. The ΔL^*-Δa^* ellipse (95% confidence) for the example.

$$f'_X(0.55) = 0.496, \quad f'_Y(0.5) = 0.529,$$

$$f'_Z(0.05) = 2.46.$$

Using Eq. (16), the covariance matrix of the errors in the CIELAB coordinates is

$$\Sigma_{L^*a^*b^*} = \begin{bmatrix} 0.094 & -0.406 & 0.162 \\ & 3.291 & -0.700 \\ & & 6.312 \end{bmatrix},$$

where the high value of $\sigma^2_{b^*}$ is due to the high value of the derivative, $f'_Z(0.05)$, and large coefficients of third row of matrix **N**. The corresponding correlation matrix is

$$\mathbf{R}_{L^*a^*b^*} = \begin{bmatrix} 1 & -0.729 & 0.211 \\ & 1 & -0.154 \\ & & 1 \end{bmatrix}.$$

Figure 3 shows the 95% confidence ellipse for the L^*, a^* parameters that results from the propagation of the uncorrelated instrument error to CIELAB. The influence of the relatively high $\sigma^2_{a^*}$ value, compared to $\sigma^2_{L^*}$, is seen in the highly elliptical shape for this example. The three-dimensional ellipsoid for the CIELAB errors is plotted in Fig. 4.

The square roots of the diagonal elements of the covariance matrix give the rms deviations for the CIELAB signals. These are listed in Table I. The common color-difference metric, ΔE^*_{ab} (Ref. 32) is the Euclidian distance

$$\Delta E^*_{ab} = \sqrt{\Delta L^{*2} + \Delta a^{*2} + \Delta b^{*2}}.$$

The expected value of ΔE^*_{ab} can be approximated as shown in Appendix I,

$$E[\Delta E^*_{ab}] \approx \sqrt{\sigma^2_{L^*} + \sigma^2_{a^*} + \sigma^2_{b^*}} - \frac{\sigma^2_p}{8(\sigma^2_{L^*} + \sigma^2_{a^*} + \sigma^2_{b^*})^{3/2}}, \quad (20)$$

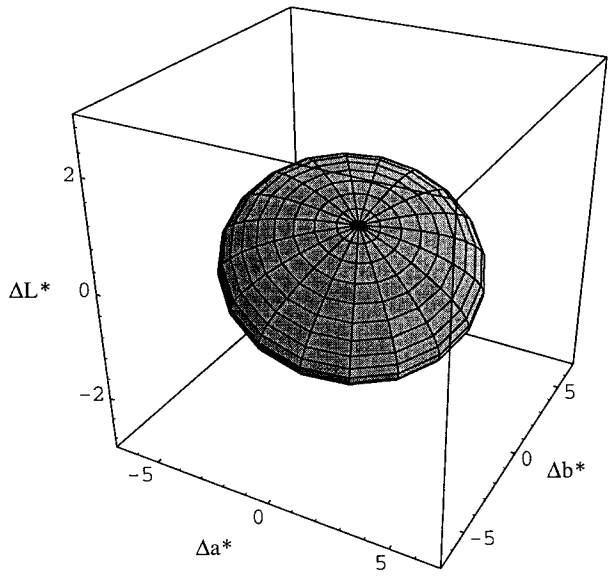

FIG. 4. L^*, a^*, b^* error ellipsoid about the mean (95% confidence) for the example.

TABLE I. CIELAB values and rms error for the example signal.

CIELAB coordinates	Mean	Standard deviation
L^*	76.07	0.31
a^*	12.81	1.81
b^*	85.06	2.51

where

$$\sigma_p^2 = 2(\sigma_{L^*}^4 + \sigma_{a^*}^4 + \sigma_{b^*}^4) - 4((\sigma_{L^*a^*})^2 + (\sigma_{L^*b^*})^2 + (\sigma_{a^*b^*})^2)$$

and was found to be equal to 2.79 for this computed example.

Note that Eq. (20) can be interpreted as describing the ΔE_{ab}^* bias due to variations in L^*, a^*, and b^*. In the absence of signal variation, $\Sigma_{L^*a^*b^*} = 0$, and, therefore, $\Delta E_{ab}^* = 0$. This is consistent with taking the 'true' CIELAB coordinate to be $\{\mu_{L^*}, \mu_{a^*}, \mu_{b^*}\}$ for the zero-mean error case considered in this example.

Following Eqs. (17) and (19), the covariance matrix for the ΔL^*, ΔC_{ab}^*, ΔH_{ab}^* error representation is

$$\Sigma_{\Delta L^*\Delta C_{ab}^*\Delta H_{ab}^*} = \begin{bmatrix} 0.094 & 0.100 & 0.426 \\ & 6.039 & 1.114 \\ & & 3.564 \end{bmatrix}. \quad (21)$$

This results in the error ellipsoid shown in Fig. 5.

The rms ΔL^*, ΔC_{ab}^*, ΔH_{ab}^* deviations for these signals are given in Table II. The values for each signal should be interpreted in terms of the units of each. For example C_{ab}^*, chroma, is in units of CIELAB distance projected onto the a^*-b^* plane. Hue angle, h_{ab}, however, is in degrees.

ΔE_{94}^*

Recently,[35] the CIE adopted the ΔE_{94}^* color-difference measure, designed to overcome some limitations of ΔE_{ab}^*. Specifically, the new measure discounts the visual color difference as the chroma of the reference color increases. This relationship can be seen from the expression,

$$\Delta E_{94}^* = \sqrt{\left(\frac{\Delta L^*}{k_L S_L}\right)^2 + \left(\frac{\Delta C_{ab}^*}{k_C S_C}\right)^2 + \left(\frac{\Delta H_{ab}^*}{k_H S_H}\right)^2}, \quad (22)$$

where

$$S_L = 1$$

$$S_C = 1 + 0.045C_{ab}^*$$

$$S_H = 1 + 0.015C_{ab}^*,$$

C_{ab}^* is the chroma of the standard, or geometric mean, and $k_L = k_C = k_H = 1$ for a set of reference sample, viewing, and illuminating conditions.

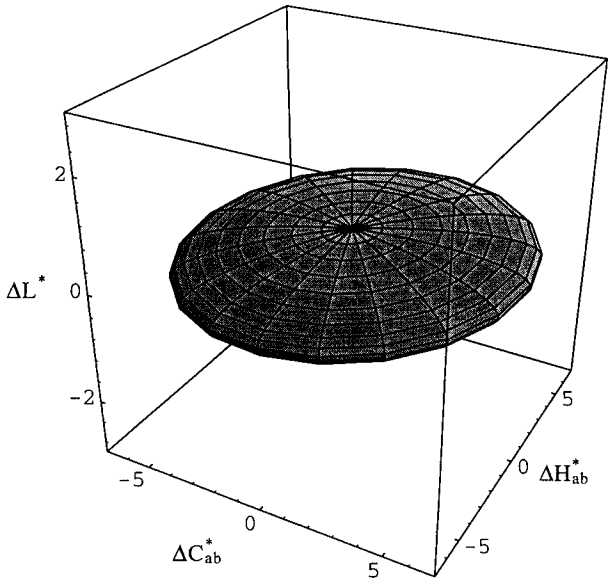

FIG. 5. ΔL^*, ΔC_{ab}^*, ΔH_{ab}^* error ellipsoid for the example color. Note unequal axes scales.

We can interpret the calculation of ΔE_{94}^* as a scaling of the ΔC_{ab}^* and ΔH_{ab}^* coordinates, so that they are transformed into a modified perceptual color space, followed by a distance computation. In matrix notation the first step is

$$\begin{bmatrix} \Delta L^* \\ \Delta C_{ab}^*/S_C \\ \Delta H_{ab}^*/S_H \end{bmatrix} = \begin{bmatrix} 1 & 0 & 0 \\ 0 & 1/(1 + 0.045C_{ab}^*) & 0 \\ 0 & 0 & 1/(1 + 0.015C_{ab}^*) \end{bmatrix} \times \begin{bmatrix} \Delta L^* \\ \Delta C_{ab}^* \\ \Delta H_{ab}^* \end{bmatrix}. \quad (23)$$

TABLE II. L^*, C_{ab}^*, ΔH_{ab}^* values and rms error for the example signal. The values of the fourth column have been scaled to conform to the ΔE_{94}^* color-difference measure.

CIELAB coordinates	Mean	Standard deviation	Scaled standard dev.
L^*	76.07	0.31	0.31
C_{ab}^*	86.02	2.46	0.51
h_{ab}^*	81.4°	—	—
ΔH_{ab}^*	—	1.89	0.82
ΔE_{ab}^*	2.79	—	—
ΔE_{94}^*	0.89	—	—

If we denote the (3 × 3) diagonal matrix of Eq. (23), evaluated where $C^*_{ab} = \mu_{C^*_{ab}}$, as **P**, then the covariance matrix for the transformed ΔL^*, ΔC^*_{ab}, ΔH^*_{ab} color space is

$$\Sigma_{L^*C^*/S_C H^*/S_H} = \mathbf{P}\Sigma_{L^*C^*H^*}\mathbf{P}^T. \quad (24)$$

This is found to be

$$\Sigma_{L^*C^*/S_C H^*/S_H} = \begin{bmatrix} 0.094 & 0.021 & 0.186 \\ & 0.255 & 0.100 \\ & & 0.680 \end{bmatrix}. \quad (25)$$

The square-root of the diagonal elements gives the rms deviations, also listed in Table II.

Following the same steps as for the calculation of $E[\Delta E^*_{ab}]$, in Eq. (20), $E[\Delta E^*_{94}]$ was found to be equal to 0.885. As expected from Eq. (22), the weighting of the variation in chroma and hue difference has been reduced. An equivalent error ellipsoid calculated from the covariance matrix of Eq. (25) is given in Fig. 6, and completes the analysis. Note that the figure is not only smaller, but more spherical than Fig. 5.

Since the error-propagation analysis described in this article is based on the first terms of the Taylor series approximation to any nonlinear transformation, the resulting statistics are necessarily approximations. Although a general investigation of the conditions necessary for accuracy of the analysis is beyond the scope of this article, we did independently investigate the computed example by simulation. This was based on the direct transformation of a set of 2000 $\{X, Y, Z\}$ coordinates to CIELAB. The normally distributed input values, generated by random number generator, had mean values and covariance matrix equal to those used in the computed example. The resulting sample covariance matrix was

$$\hat{\Sigma}_{L^*C^*/S_C H^*/S_H} = \begin{bmatrix} 0.095 & 0.025 & 0.187 \\ & 0.268 & 0.111 \\ & & 0.685 \end{bmatrix}.$$

This compares favorably with the calculated matrix of Eq. (25), as does the computed sample mean, $\overline{\Delta E^*_{94}} = 0.898$, with the previously calculated value of 0.885.

DETECTOR ERROR SPECIFICATION

The above computed example illustrates how the error propagation analysis can be applied to color-signal transformations, and CIELAB error statistics can be predicted from the input signal, $\{X, Y, Z\}$, mean vector, and covariance matrix. We can also use these techniques to propagate errors from CIELAB (back) to tristimulus values or camera signals, if the matrix operations and the nonlinear transformations are invertible. This will now be outlined.

For a measurement system we are given an error budget such that no more than a given average error, ΔE^*_{ab}, in CIELAB is allowable due to stochastic error in the input tristimulus-value signals. The calculations of ΔE^*_{ab} and

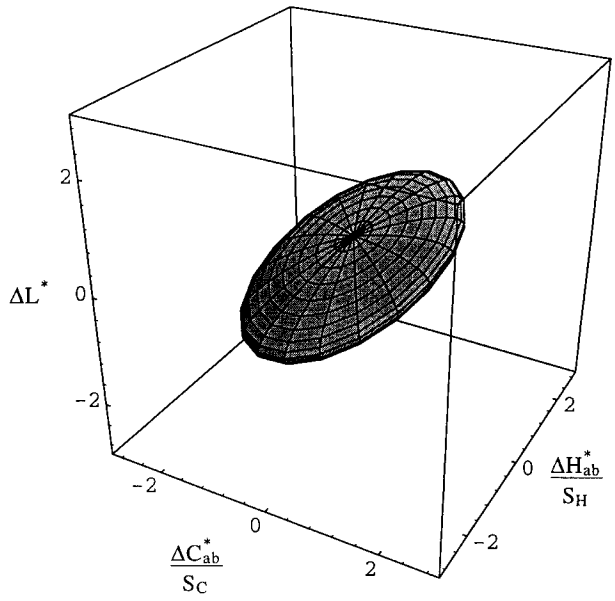

FIG. 6. Error ellipsoid based on transformed $\Delta L^*, \Delta C^*_{ab}, \Delta H^*_{ab}$ coordinates, consistent with the ΔE^*_{94} color-difference measure.

ΔE^*_{94} cannot be inverted. We can choose, however, to evaluate the propagation of CIELAB errors with a given form of covariance matrix. In addition, due to the nonlinear step in the transformation, the error propagation will depend on the mean value of the signal to be evaluated, as was the case for the transformation $\{X, Y, Z\} \rightarrow \{L^*, a^*, b^*\}$. As an example, the same mean signal will be used as for the previous case, and, for simplicity, we let the acceptable errors have a mean $E[\Delta E^*_{94}] = 0.5$, and assume independent errors in L^*, a^*, and b^*. From Eq. (20), setting the covariance terms to zero,

$$\Sigma_{\Delta L^*\Delta C^*_{ab}/S_C \Delta H^*_{ab}/S_C} = \frac{(E[\Delta E^*_{94}])^2}{3}\mathbf{I} = 0.083\mathbf{I}. \quad (26)$$

As in Eq. (5),

$$\Sigma_{\Delta L^*\Delta C^*_{ab}\Delta H^*_{ab}} = \mathbf{P}^{-1}\Sigma_{\Delta L^*\Delta C^*_{ab}/S_C \Delta H^*_{ab}/S_C}[\mathbf{P}^{-1}]^T,$$

where **P** is given in Eq. (23). The next steps are the transformation from $\{\Delta L^*, \Delta C^*_{ab}, \Delta H^*_{ab}\}$ to $\{\Delta L^*, \Delta C^*_{ab}, \Delta h_{ab}\}$ and then to $\{L^*, a^*, b^*\}$. Since the matrices $J_{L^*C^*_{ab}h^*_{ab}}$, $J_{L^*a^*b^*}$, and $J_{f(t)}$ are easily inverted, we can write the error covariance matrix for the input signals as

$$\Sigma_t = J^{-1}_{f(t)}J^{-1}_{L^*a^*b^*}J^{-1}_{L^*C^*_{ab}h^*}\Sigma_{\Delta L^*\Delta C^*_{ab}\Delta H^*_{ab}} \times [J^{-1}_{L^*C^*_{ab}h^*}J^{-1}_{L^*a^*b^*}J^{-1}_{f(t)}]^T. \quad (27)$$

For the example signal, the calculated tristimulus-value covariance matrix is

$$\Sigma_t = 10^{-5}\begin{bmatrix} 3.28 & 2.36 & 0.322 \\ & 2.21 & 0.477 \\ & & 0.908 \end{bmatrix} \quad (28)$$

and the rms signal error of

$$\sigma_X = 0.0057,\ \sigma_Y = 0.0047,\ \sigma_Z = 0.0030.$$

Equation (28) represents the propagation of the covariance matrix of Eq. (26) to an equivalent input colorimeter/camera signal matrix. This means that, for independent CIELAB errors, to achieve an average ΔE^*_{94} value of 0.5, the source error covariance elements must be no greater than those given in Eq. (28).

CONCLUSIONS

From the general analysis of error propagation, the first two statistical moments of stochastic errors can be analyzed in many current color-spaces and through many color-image processing transformations. In addition to the magnitude of the signal variance, the propagation of the covariance between sets of signals has been described. The methods used have been implemented using matrix-type operations, but there are several requirements for their success. The errors to be analyzed must result from continuous stochastic sources. If so, the expression for the linear matrix transformation, Eq. (5), is exact. The expressions for nonlinear transformations, however, are based on truncated series approximations. The partial derivatives included in these expressions should be continuous. We note, however, as shown for the tristimulus values-CIELAB path, that approximately continuous transformations can also be analyzed.

The accuracy of the linear approximations can be evaluated by examining the higher-order derivatives. For example, the magnitude of the second term of the RHS of Eqs. (2) or (3) should be much less than the first, $f'^2_x \sigma^2_x$, in order to use the linear approximation of Eqs. (4) and (7). Since both f'_x and f''_{xx} are functions of μ_x, it is useful to identify values of the argument(s) for which the condition does not hold, e.g., $f'_x \cong 0$. If the first derivative is small compared to the second, and the error distribution is approximately Gaussian, then Eq. (3) can be used. This form can also be used for error distributions that are similar in shape to the normal, e.g., lognormal and Laplacian. For other distributions, such as the uniform, chi-square, or exponential, Eq. (3) should be used.

By applying the error propagation techniques, variation due to measurement precision can be compared with the effects of experimental variables using error ellipses and ellipsoids. These are based on the calculated or observed covariance matrices and underlying probability density functions, and require the analysis of covariance. We can also address the inverse of many color-signal transformations of current interest. As demonstrated, a given tolerance of average ΔE^*_{ab} or ΔE^*_{94} can be related to an equivalent uncertainty in tristimulus values, other sets of detected signals, or image pixel values.

ACKNOWLEDGEMENTS

We thank Seth Ansell with Hewlett-Packard, and Richard Alfin of Eastman Kodak Company for *Mathematica* programs on which we based our error-ellipsoid computation. In addition, the comments of anonymous reviewers are appreciated.

APPENDIX I: EXPECTED VALUE OF ΔE^*_{ab}

The expected value of ΔE^*_{ab} is

$$\mathrm{E}[\Delta E^*_{ab}] = \mathrm{E}[\sqrt{\Delta L^{*2} + \Delta a^{*2} + \Delta b^{*2}}], \quad (A1)$$

where $\Delta L^* = L^* - \mu_{L^*}$, etc. Since the first and second partial derivatives of the function $\Delta E^*_{ab}(L^*, a^*, b^*)$ are undefined when evaluated at $L^* = a^* = b^* = 0$, a key requirement of error propagation based on Taylor series is violated. We can, however, approximate equation (A1) in two steps and compare the result with that for a simple univariate case. We include up to the fourth moment.

First let

$$p = L^{*2} + a^{*2} + b^{*2},$$

where L^*, a^*, and b^* now represent the zero-mean random variables, ΔL^*, Δa^*, Δb^*, with some covariance matrix, $\Sigma_{L^*a^*b^*}$. The expected value of p is

$$\mathrm{E}[p] = \mu_p = \sigma^2_{L^*} + \sigma^2_{a^*} + \sigma^2_{b^*}. \quad (A2)$$

The variance is

$$\sigma^2_p = \mathrm{E}[p^2] - \mu^2_p. \quad (A3)$$

If we expand p^2 and take expectations,

$$\mathrm{E}[p^2] = \mathrm{E}[L^{*4}] + \mathrm{E}[a^{*4}] + \mathrm{E}[b^{*4}] + 2[\mathrm{E}[L^{*2}a^{*2}] + \mathrm{E}[L^{*2}b^{*2}] + \mathrm{E}[a^{*2}b^{*2}]]. \quad (A4)$$

The terms of Eq. (A4) cannot be related to $\Sigma_{L^*a^*b^*}$ without an assumption about the probability density function, $P(L^*,a^*,b^*)$. If we can approximate this by a joint normal distribution, then

$$\mathrm{E}[L^{*4}] = 3\sigma^4_{L^*}, \qquad \mathrm{E}[L^{*2}a^{*2}] = \sigma^2_{L^*}\sigma^2_{a^*} + 2(\sigma_{L^*a^*})^2, \cdots \quad (A5)$$

Substituting Eqs. (A5) and (A4) into (A3),

$$\sigma^2_p = 2(\sigma^4_{L^*} + \sigma^4_{a^*} + \sigma^4_{b^*}) + 4[(\sigma_{L^*a^*})^2 + (\sigma_{L^*b^*})^2 + (\sigma_{a^*b^*})^2]. \quad (A6)$$

Next we form the transformed variable,

$$q = \sqrt{p}.$$

Here we can expand the function in a series about the mean value of p, which is not zero. Following this approach, the expected value is given by

$$E[q(p)] = E[\Delta E^*_{ab}] \approx \sqrt{\sigma^2_{L^*} + \sigma^2_{a^*} + \sigma^2_{b^*}} - \frac{\sigma^2_p}{8(\sigma^2_{L^*} + \sigma^2_{a^*} + \sigma^2_{b^*})^{3/2}}, \quad \text{(A7)}$$

where σ^2_p is given by Eq. (A6).

Univariate Normally Distributed Errors

As stated above, Eq. (A1) does not have continuous partial first derivatives when $\mu_{L^*} = \mu_{a^*} = \mu_{b^*} = 0$. To compare our approximation, Eq. (A7), with a known result, consider the case of a normally distributed error in only one variable, i.e., where $\sigma^2_{a^*} = \sigma^2_{b^*} = 0$. Equation (A7) becomes

$$E[\Delta E^*_{ab}] = 0.75\sigma_{L^*}.$$

For this case, however, ΔE^*_{ab} is seen as merely the absolute value of ΔL^*. The expected value of Eq. (A1) is the mean absolute deviation given, for a normal random variable,[36] by $0.80\sigma_{L^*}$. So, for this univariate case, using Eq. (A7) underestimates the mean of ΔE^*_{ab}. A less accurate, but more conservative approximation is given by the first term of Eq. (A7), resulting in $E[\Delta E^*_{ab}] = \sigma_{L^*}$.

1. I. Nimeroff, Propagation of errors in spectrophotometric colorimetry. *J. Opt. Soc. Am.* **43,** 531–533 (1953).
2. I. Nimeroff, Propagation of errors in tristimulus colorimetry. *J. Opt. Soc. Am.* **47,** 697–702 (1957).
3. I. Nimeroff, Comparison of uncertainty ellipses calculated from two spectrophotometric colorimetry methods by an automatic-computer program. *J. Opt. Soc. Am.* **56,** 230–237 (1966).
4. I. Nimeroff, J. R. Rosenblatt, and M. D. Dannemiller, Variability of spectral tristimulus values. *J. Opt. Soc. Am.* **52,** 685–692 (1962), also published by the same title in *J. Res. Nat. Bur. Stand.* **65A,** 475–483 (1961).
5. A. K. Kustarev, Colorimetric implications of spectrophotometric errors. *Svetotekhnika* **12,** 7–9 (1984) (in Russian).
6. V. I. Lagutin, Estimating errors in determining color coordinates (in Russian). *Izmer. Tekh.* **2,** 27–29 (1987), translated in *Meas. Tech.,* Plenum Publishing Corp. **30,** 150–163 (1987).
7. A. R. Robertson, Colorimetric significance of spectrophotometric errors. *J. Opt. Soc. Am.* **57,** 691–698 (1967).
8. M. D. Fairchild and L. Reniff, Propagation of random errors in spectrophotometric colorimetry. *Color Res. Appl.* **16,** 361–367 (1991).
9. J. C. Dainty and R. Shaw, *Image Science,* Academic Press, London, 1974, pp. 152–182, 232–317.
10. F. O. Huck, C. L. Fales, N. Halyo, and W. Sams, Image gathering and processing: Information and fidelity. *JOSA A* **2,** 1644–1665 (1985).
11. P. D. Burns, Image modulation and noise characteristics of laser printers. *J. Imaging Sci.* **31,** 74–81 (1987).
12. P. D. Burns, Signal-to-noise ratio analysis of charge coupled device imagers. *Proc. SPIE* **1242,** 187–194 (1990).
13. A. J. Ahumada, Putting the visual system noise back in the picture. *J. Opt. Soc. Am. A* **4,** 2372–2378 (1987).
14. E. I. Stearns, Influence of spectrophotometer slits on tristimulus calculations. *Color Res. Appl.* **6,** 78–84 (1981).
15. E. I. Stearns and R. E. Stearns, An example of a method for correcting radiance data for bandpass error. *Color Res. Appl.* **13,** 257–259 (1988).
16. R. S. Berns and K. H. Petersen, Empirical modeling of systematic spectrophotometric errors. *Color Res. Appl.* **13,** 243–256 (1988).
17. A. Papoulis, *Probability, Random Variables and Stochastic Processes,* McGraw–Hill, New York, 1965, pp. 151–152.
18. G. E. P. Box, W. G. Hunter, and J. S. Hunter, *Statistics for Experimenters,* Wiley, New York, 1978, pp. 87–89.
19. K. M. Wolter, *Introduction to Variance Estimation,* Springer–Verlag, New York, 1985, pp. 221–229.
20. B. N. Taylor and C. E. Kuyatt, *Guidelines for evaluating and expressing the uncertainty of NIST measurement results, NIST Tech. Note 1297,* US Dept. of Commerce, Washington, 1993, p. 8.
21. P. Hung, Color rendition using three-dimensional interpolation. *Proc. SPIE* **1909,** 111–115 (1988).
22. J. M. Kasson, S. I. Nin, W. Plouffe, and J. L. Hafner, Performing color space conversions with three-dimensional linear interpolation. *J. Electron. Imaging* **4,** 226–250 (1995).
23. E. Allen, Matrix algebra for colorimetrists. *Color Eng.* **4,** 24–31 (1966).
24. T. Jaaskelainen, J. Parkkinen, and S. Toyooka, Vector-subspace model for color representation. *J. Opt. Soc. Am. A* **7,** 725–730 (1990).
25. H. J. Trussell, Applications of set theoretic methods to color systems. *Color Res. Appl.* **16,** 31–41 (1991).
26. J. A. Quiroga, J. Zoido, J. Alonso, and E. Bernabeu, Colorimetric matching by minimum-square-error fitting. *Appl. Opt.* **33,** 6139–6141 (1994).
27. R. A. Johnson and D. W. Wichern, *Applied Multivariate Statistical Analysis,* Prentice–Hall, Engelwood Cliffs, New Jersey, 1992, pp. 61–62.
28. G. Wyszecki and W. S. Stiles, *Color Science: Concepts and Methods, Quantitative Data and Formulae,* 2nd Ed., Wiley, New York, 1982, pp. 328–330.
29. B. Sluban and J. H. Nobbs, The Colour Sensitivity of a Colour Matching Recipe. *Color Res. Appl.* **20,** 226–234 (1995).
30. R. R. Searle, *Matrix Algebra Useful for Statistics,* Wiley, New York, 1982, p. 338.
31. ASTM, Standard Test Method for Computing the Colors of Objects by Using the CIE System, *E308-95. ASTM Standards on Color and Color Appearance,* 5th Ed., American National Standards Institute, West Conshohocken, 1996, pp. 253–282.
32. *ibid.,* pp. 265, 10-nm weights.
33. CIE, Colorimetry, *CIE Publication No. 15.2,* 2nd Ed., CIE Central Bureau, Vienna, 1986, pp. 30–32.
34. Ref. 27, pp. 126–133.
35. CIE Industrial color-difference evaluation, *Technical Report Number CIE 116-1995,* CIE Central Bureau, Vienna, 1995.
36. Ref. 17, p. 147.